http://dx.doi.org/10.5012/bkcs.2012.33.11.3581

Spectral, Electrochemical, Fluorescence, Kinetic and *Anti*-microbial Studies of Acyclic Schiff-base Gadolinium(III) Complexes

A. Vijayaraj, R. Prabu, R. Suresh, R. Sangeetha Kumari,[†] V. Kaviyarasan,[†] and V. Narayanan[*]

Department of Inorganic Chemistry, School of Chemical Sciences, University of Madras, Guindy Maraimalai Campus, Chennai 600 025, India. [*]E-mail: vnnara@yahoo.co.in
[†]Centre for Advanced Studies in Botany, University of Madras, Guindy Maraimalai Campus, Chennai 600 025, India
Received June 5, 2012, Accepted August 1, 2012

A new series of acyclic mononuclear gadolinium(III) complexes have been prepared by Schiff-base condensation derived from 5-methylsalicylaldehyde, diethylenetriamine, tris(2-aminoethyl) amine, triethylenetetramine, *N,N*-bis(3-aminopropyl)ethylene diamine, *N,N*-bis(aminopropyl) piperazine, and gadolinium nitrate. All the complexes were characterized by elemental and spectral analyses. Electronic spectra of the complexes show azomethine (CH=N) within the range of 410-420 nm. The fluorescence efficiency of Gd(III) ion in the cavity was completely quenched by the higher chain length ligands. Electrochemical studies of the complexes show irreversible one electron reduction process around −2.15 to −1.60 V The reduction potential of gadolinium(III) complexes shifts towards anodic directions respectively upon increasing the chain length. The catalytic activity of the gadolinium(III) complexes on the hydrolysis of 4-nitrophenylphosphate was determined. All gadolinium(III) complexes were screened for antibacterial activity.

Key Words : Schiff-base ligands, Gadolinium(III) complexes, Fluorescence, Kinetic, *Anti*-microbial

Introduction

In the past decade, a great attention has been devoted to the design and the synthesis of macrocyclic ligands and their lanthanide complexes are a fascinating area of research, owing to their importance in basic and applied chemistry. In particular, acyclic Schiff bases have successfully been proposed as excellent systems in the formation of mono, homo, hetero nuclear lanthanide complexes.[1,2] Detailed investigations of their stereo chemical, electronic, magnetic, and catalytic properties have allowed the proposal of new, highly efficient molecular devices or probes for a number of specific applications.

Much of the research on the chemistry of lanthanide(III) metal ions in recent years has focused on their potential uses in bioinorganic chemistry and materials science.[3] One of the most important applications is the use of Gd(III) complexes for magnetic resonance imaging (MRI)[4,5] anionic Gd(III) complexes are potentially useful as MRI contrast agents with low toxicity.[6]

Mononuclear complexes of rare earth ions have considerable attention because of their electronic and nuclear properties which are of great interest in luminescent,[7] as a catalysts for RNA cleavage,[8] radioimmunotherapy, radioimmunoscintigraphy, as NMR shift reagents,[9,10] as NMR shift and relaxation agents for proteins[11] and biological cations and, luminescent computational logic gates.[12] Sequestration and subsequent transportation of rare earth metal ions based Schiff base complexes have good thermodynamic stability and kinetic inertness toward metal dissociation. Therefore, there is sustained interest towards the design of multidentate ligands capable of forming stable Ln(III) complexes for solution applications.[13] Freire *et al.*[14] reported the fluorescence activity of Gd(III) Schiff base complexes, salen type of aldehydes with aromatic diamine. In this paper, we reported the preparation of mononuclear Gd(III) Schiff base complexes with influence of the ligands modification on spectral, electrochemical, fluorescence, life time measurement, kinetic and antimicrobial activity of the complexes.

Experimental

Chemicals and Reagents. 5-Methylsalicylaldehyde[15] was prepared following the literature method. Analytical grade methanol, acetonitrile and dimethyl formamide were purchased from Qualigens. TBAP (tetra(*n*-butyl)ammonium perchlorate) used as supporting electrolyte in electrochemical measurements was purchased from Fluka and recrystallized from hot methanol. $Gd(NO_3)_3{\cdot}5H_2O$ was purchased from Chemical Drug House, *N,N*-bis-(3-aminopropyl) piperazine, *N,N*-bis-(3-aminopropyl) ethylene diamine and tris-(2-aminoethyl)amine were purchased from Aldrich. Triethylenetetramine and diethylenetriamine were purchased from Qualigens.

Microorganisms. The test bacterial strains *Pseudomonas aeruginosa*, *Klebsiella* sp, *Candida albicans*, *Salmonella typhi*, and *Salmonella enterica serovar Paratyphi A* were obtained from the Department of Microbiology, SRM Medical University, Chennai, Tamil Nadu was isolated clinically. The test organisms were sub-cultured at 37 °C and maintained on nutrient agar media.

Physical Measurements. Elemental analyses of the complexes were obtained using a Haereus CHN rapid analyzer. IR spectra were recorded on a PerkinElmer FT-IR 8300 series spectrophotometer on KBr disks from 4000 to 400

cm^{-1}. ^1H NMR spectra were recorded using a JEOL GSX 400 MHz NMR spectrometer. ESI Mass spectra were obtained on a JEOL DX-303 mass spectrometer. Electronic spectral studies were carried out on a PerkinElmer 320 spectrophotometer. Steady state fluorescence measurements were carried out by using a fluorescence spectrophotometer (Fluoromax 4P, Horiba Jobin Yvon). Stock solutions of 3×10^{-5} M in DMF medium were used for fluorescence measurements. The fluorescence decay curve and lifetime measurements were carried out using a time correlation single-photon counting spectrometer (IBH, model 5000U). The excitation source was 280 nm nano LED (IBH) with a pulse width of < 1 ns. The fluorescence emission was monitored at a right angle to the excitation path, and photons were detected by a MCP-PMT (Hamamatsu, model R3809U) detector. The data analysis was carried out by the software provided by IBH (DAS-6), which is based on deconvolution techniques using the nonlinear least-squares method.

Cyclic voltammograms were obtained on a CHI-600A electrochemical analyzer under oxygen-free conditions using a three-electrode cell in which a glassy carbon electrode was the working electrode, a saturated Ag/AgCl electrode was the reference electrode and platinum wire was the auxiliary electrode. A ferrocene/ferrocenium couple was used as an internal standard and $E_{1/2}$ of the ferrocene/ferrocenium (Fc/Fc^+) couple under the experimental condition was 470 mV. Tetra(*n*-butyl)ammonium perchlorate (TBAP) 1×10^{-1} M was used as the supporting electrolyte. Catalytic hydrolysis of 4-nitrophenylphosphate by the Gd(III) complexes was monitored by following the UV-vis absorbance change at 420 nm (assigned to the 4-nitrophenolate anion) as a function of time. A plot of log ($A_\infty/A_\infty - A_t$) *vs* time was made for each complex and the rate constants for the catalytic oxidations and the hydrolysis of 4-nitrophenylphsophate were calculated.

Preparation of Metal Complexes.

[Gd(III)L^1](H$_2$O): Ligands, L^1, L^2, L^3, L^4, and L^5 were synthesized by our previous reports.[16,17] In order to prepare metal complexes, an absolute methanol solution containing $Gd(NO_3)_3 \cdot 5H_2O$ (45 mg, 0.1 mmol) was added drop-wise to a solution of L^1 (33.9 mg, 0.1 mmol) in 20 mL of absolute methanol under constant stirring condition. After refluxing for 8 h, the yellow colour microcrystal were obtained, which was filtered and washed with methanol followed by diethyl ether and dried in vacuum. The obtained complex was recrystallized from methanol/acetonitrile (1:3). The above reactions have shown in Scheme 1.

Yield: 41.3 mg, (51.2%) Analytical data for $C_{20}H_{24}N_5O_8Gd$: Calc. (M.Wt: 620.08): C, 38.76; H, 3.90; N, 11.30; Gd, 25.38. Found: C, 37.78; H, 3.69; N, 10.11; Gd, 24.83%. Selected IR (KBr) (ν/cm^{-1}): 1125 ν(C-O), 1478 s [ν(N=O)], 1296 s [$\nu_{asym}(NO_2)$], 1051s [$\nu_{sym}(NO_2)$], 1631 ν(C=N), 630 ν(M-N), 440 ν(M-O), ESI-MS in CH_3OH: *m/z*: $[Gd(III)L^1(NO_3)_2]^-$ (618.08).

Preparation of Complex [Gd(III)L^2]: [Gd(III)L^2] was synthesized by following the previously described procedure for [Gd(III)L^1], using (L^2) ligand (38 mg, 0.1 mmol) instead of (L^1) ligand. The yellow color complex was obtained. Yield: 31.3 mg, (48.2%) Analytical data for $C_{22}H_{28}N_5O_5Gd$: Calc. (M.Wt: 599.73): C, 39.81; H, 4.56; N, 12.66; Gd, 23.69. Found: C, 39.22; H, 4.08; N, 11.03; Gd, 23.07. Selected IR (KBr) (ν/cm^{-1}): 1127 ν(C-O), 1478 s [ν(N=O)], 1315 s [$\nu_{asym}(NO_2)$], 1101 s [$\nu_{sym}(NO_2)$], 1631 ν(C=N), 626 ν(M-N), 443 ν(M-O), ESI-MS in CH_3OH: *m/z*: [Gd(III)L^2(NO_3)] (598.73).

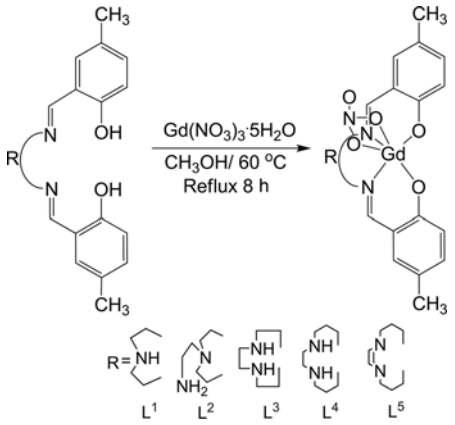

Scheme 1. Schematic diagram for the synthesis of [Gd(III)L^1-L^5] Complexes.

Preparation of Complex [Gd(III)L^3]: [Gd(III)L^3] was synthesized by following the previously described procedure for [Gd(III)L^1], using (L^3) ligand (38.2 mg, 0.1 mmol) instead of (L^1) ligand. The yellow color complex was obtained. Yield: 28.3 mg, (39.2%) Analytical data for $C_{22}H_{26}N_5O_5Gd$: Calc. (M.Wt: 597.72): C, 62.24; H, 6.83; N, 12.70; Gd, 23.16. Found: C, 62.15; H, 6.75; N, 12.13; Gd, 22.96. Selected IR (KBr) (ν/cm^{-1}): 1136 ν(C-O), 1475 s [ν(N=O)], 1314 s [ν_{asym} (NO_2)], 1103 s [ν_{sym} (NO_2)], 1630 ν(C=N), 664 ν(M-N), 453 ν(M-O), ESI-MS in CH_3OH: *m/z*: [Gd(III)L^3(NO_3)] (598.14).

Preparation of Complex [Gd(III)L^4]: [Gd(III)L^4] was synthesized by following the previously described procedure for [Gd(III)L^1], using (L^4) ligand (42.6 mg, 0.1 mmol) instead of (L^1) ligand. The yellow color complex was obtained. Yield: 48.3 mg, (62.2%) Analytical data for $C_{24}H_{30}N_5O_5Gd$: Calc. (M.Wt: 626.17): C, 63.26; H, 7.58; N, 12.54; Gd, 22.58. Found: C, 62.66; H, 7.30; N, 11.82; Gd, 22.44. Selected IR (KBr) (ν/cm^{-1}): 1149 ν(C-O), 1453 s [ν(N=O)], 1353 s [$\nu_{asym}(NO_2)$], 1042 s [$\nu_{sym}(NO_2)$], 1635 ν(C=N), 556 ν(M-N), 460 ν(M-O), ESI-MS in CH_3OH: *m/z*: [Gd(III)L^4(NO_3)] (623.20).

Preparation of Complex [Gd(III)L^5]: [Gd(III)L^5] was synthesized by following the previously described procedure for [Gd(III)L^1], using (L^5) ligand (46.8 mg, 0.1 mmol) instead of (L^1) ligand. The yellow color complex was obtained. Yield: 33.3 mg, (58.2%) Analytical data for $C_{26}H_{34}N_5O_5Gd$: Calc. (M.Wt: 653.83): C, 64.62; H, 7.59; N, 11.71; Gd, 21.91. Found: C, 64.11; H, 7.41; N, 11.01; Gd, 21.01. Selected IR (KBr) (ν/cm^{-1}): 1130 ν(C-O), 1492 s [ν(N=O)], 1353 s [$\nu_{asym}(NO_2)$], 1161 s [$\nu_{sym}(NO_2)$], 1631 ν(C=N), 534 ν(M-N), 458 ν(M-O), ESI-MS in CH_3OH: *m/z*: [Gd(III)L^5(NO_3)] (655.13).

Results and Discussion

FT IR Spectral Analysis. The FT IR spectrum of the precursor compound 5-methylsalicylaldehyde (PC) shows a sharp band at around 1655 cm^{-1} due to the presence of CHO group. The OH group in the ligand shows a broad peak at 3378 cm^{-1}. All the ligands show a band at 3389 cm^{-1} due to the phenolic OH groups. After the complexation, phenolic -OH peak disappears which is due to deprotonation followed by coordination of the ligands to the Gd(III) metal ion. The band in the region of 1590-1636 cm^{-1} in the ligands is due to the presence of imine(C=N) group. All the complexes shows a sharp band in the region 1629-1636 cm^{-1}, due to νC=N stretching. The complete disappearance of (C=O) group of the precursor and the appearance of imine (CH=N-) group in the ligands shows the effective Schiff base condensation between the aldehyde group of the precursor compound and the amine groups. The bands at 1432 and 1492 cm^{-1} are due to ν(N=O) (ν_1) and $\nu_{asym}(NO_3^-)$ vibration (ν_5) of coordinated nitrates. The $\nu_{asym}(NO_3^-)$ vibration (ν_2) at 1051 cm^{-1} is characteristic of a bidentate nitrate group. The separation of the ν_1 and ν_5 modes has been used as a criterion to distinguish between the mono-and bi-dentate chelating nitrates coordinated to gadolinium(III) metal ion. Sharp peaks observed around 1330-1400 cm^{-1} are assigned due to ν(Gd-NO_3) in the complexes.[18] For the complexes, bands at 420-460 cm^{-1} could be assigned to -(M–O) bond. Other weak bands at lower frequency could be assigned to (M–N) bond. The spectra of all the complexes are dominated by bands at 3150-3070 cm^{-1} which are due to the aromatic C-H stretching vibration. The appearance of new bands in the region of 1125-1149 cm^{-1} in all the complexes, suggests the formation of phenoxide bridge between ligand and metal ions. FT-IR spectra are given in supplementary as Figure S1.1 to S1.5

Mass Spectral Analysis. The ESI mass spectra of mono nuclear [Gd(III)L^4] and [Gd(III)L^5] complex shows the molecular ion peak (M^+), (M^-) at *m/z* = 623.20 and 655.13 respectively. The ESI-MS data show the molecular ion peak indicating the stability of the structure in a solution phase. The spectra also contain peaks due to molecular anion and cations. The spectra show some prominent peaks corresponding to the various fragments of the complexes. The ESI mass spectra are given in supplementary as Figures S2.1 & S2.2.

Electronic Spectral Analysis. The electronic spectra of the complexes were recorded in DMF. The electronic spectra of the complexes are shown in Figures 1 and the data are tabulated in Table 1. The electronic spectra of the complexes were observed as three main transitions. The strong bands observed in the range 250-280 nm is due to (π-π*) associated with intra ligands transition. A moderate intense band observed in the range of 310-340 nm is due to (n-π*) associated with ligand to metal charge transfer transition.[19] A weak band observed in the range 410-420 nm is due to azomethine CH=N chromophore coordinated to the [Gd(III)] metal ion through the nitrogen atom. It is possible that *f*-orbital of the metal ion and the *p*-orbital of H_2L overlap each other to form a greater conjugated system after enolizing and complexing.[20] The electronic spectral studies inferred that a decrease in λ_{max} (blue shift) of the (n-π*) transition of the Gd(III) ion in the complexes Gd(III)L^1-L^5 indicates that the coordination geometry around the Gd(III) atom of the complexes is more distorted. This is due to the flexibility of the macrocyclic ring upon increasing the chain length of the imine compartment, which causes more distortion of the geometry. The coordination number of gadolinium(III) is nine, and its coordination geometry is a distorted mono-capped square antiprisms.

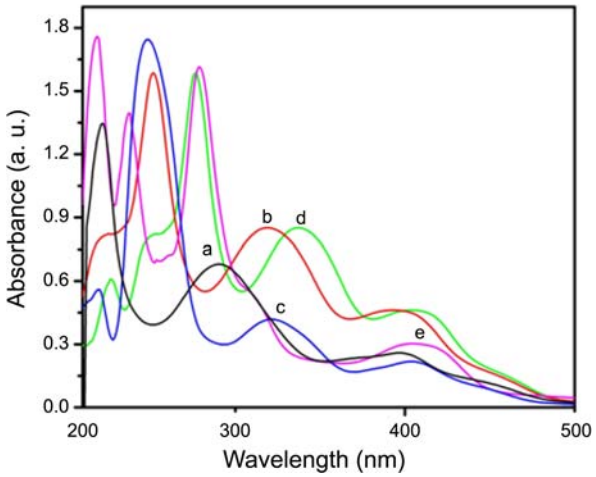

Figure 1. Electronic Spectra of mono nuclear [Gd(III)L^1-L^5] complexes. (a) [Gd(III)L^1], (b) [Gd(III)L^2], (c) [Gd(III)L^3], (d) [Gd(III)L^4] and (e) [Gd(III)L^5].

Table 1. Electronic spectral data of acyclic mononuclear [Gd(III)L^1-L^5] complexes

Complexes	λ_{max} (nm) (ε/M^{-1} cm^{-1})	
	C=N	charge transfer
[Gd(III)L^1]	410(16732)	340(15480), 280(22650)
[Gd(III)L^2]	420(15456)	330(11985), 260 (23900)
[Gd(III)L^3]	420(15449)	335(11455), 250(24350)
[Gd(III)L^4]	415(16420)	335(11680), 250(24340)
[Gd(III)L^5]	420(15432)	310(13985), 270(22950)

Fluorescent Properties of Complexes [Gd(III)L^1-L^5]. Emission spectrum of the [Gd(III)L^1-L^5] complexes recorded in DMF solution with excitation at 400 nm is shown in Figure 2. The luminescence of Ln^{3+} chelates is related to the efficiency of the intramolecular energy transfer between the triplet levels of the ligand and the emitting level of the ions, which depends on the energy gap between the two levels. In the intramolecular energy transfer, triplet state energy of the ligand is regarded as an important factor in excitation of the lanthanide ion.[21,22] Comparing with this mononuclear [Gd(III)L^1-L^5] complexes. [Gd(III)L^5] exhibit lower emission band in the range 400-600 nm indicating the fluorescence of Gd(III) ion in the cavity was partly quenched by the higher chain length ligands. The intensity of the peak around 700 nm is affected to a greater extent compared to lower wavelength emission peak due to coordination environment. All

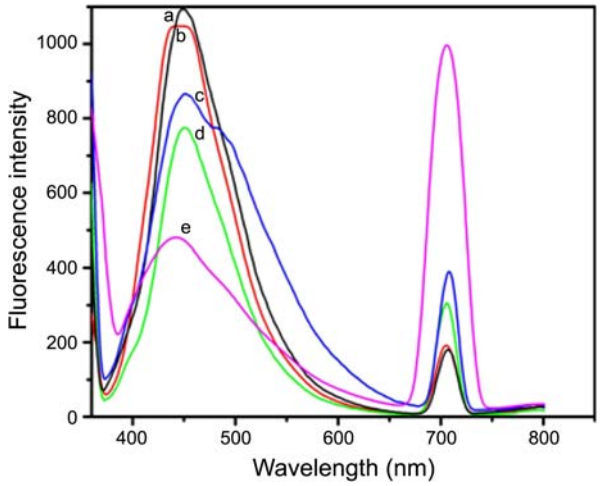

Figure 2. Fluorescence spectra of [Gd(III)L^1-L^5] complexes (a) [Gd(III)L^1], (b) [Gd(III)L^2], (c) [Gd(III)L^3], (d) [Gd(III)L^4] and (e) [Gd(III)L^5].

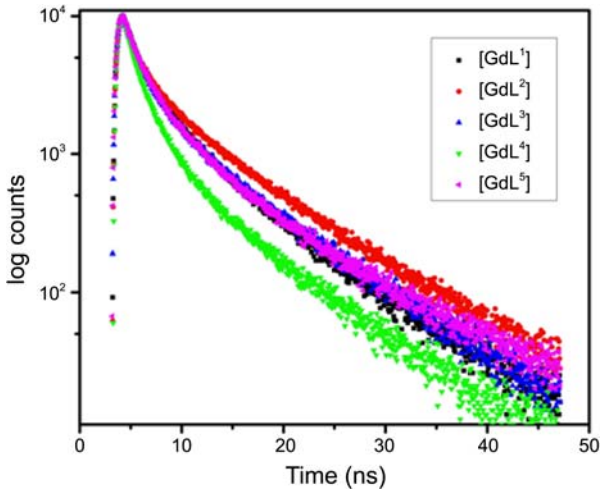

Figure 3. Life time decay of [Gd(III)L^1-L^5] complexes. (a) [Gd(III)L^1], (b) [Gd(III)L^2], (c) [Gd(III)L^3], (d) [Gd(III)L^4] and (e) [Gd(III)L^5].

emissions arise from the ^6D_j level corresponding to the $^6D_j \leftarrow {}^8S_{7/2}$ ($\Delta J = 0$, 1-4) transition. The weak band at 460 nm arises from the $^6D_j \leftarrow {}^8S_{7/2}$ transition. The band around 470 nm for $^6D_j \leftarrow {}^8S_{7/2}$, which is magnetic-dipole allowed, is hardly affected by a change of the coordination environment. The intense band around 710 nm for $^6D_j \leftarrow {}^8S_{7/2}$ is an electric-dipole allowed transition and its emission intensity is sensitive to the coordination environment of Gd(III). The fluorescence spectra show a forbidden transition, $^6D_j \leftarrow {}^8S_{7/2}$ and a hypersensitive transition, $^6D_j \leftarrow {}^8S_{7/2}$ which are expected for the noncentrosymmetric coordination environment. This shows that fluorescence emission of Gd(III) ions in the complex was influenced by the nature of the ligand.

Life Time Measurement of [Gd(III)L^1-L^5] Complexes. Advances in the design and miniaturization of the lasers and electronics required for Time Correlated Single Photon Counting (TCSPC) measurement of fluorescence lifetime have simplified the use of the time domain method. This fitting clearly shows that the complexes are well fitted with tri exponential fitting. The emission spectra and decay time measurements for the [Gd(III)L^1] to [Gd(III)L^5] complexes allowed the identification of the highest ligand triplet state which is shown in Figure 3. It can be seen that the [Gd(III)L^5] complex has longer life time.

The lifetime decay curve for all [Gd(III)L^1-L^5] complexes are tri exponential and the data are given in Table 2. The exponential decay behavior depends on the number of different luminescent centre, energy transfer, defects and impurities in the host.

Electrochemistry of the Complexes.

Reduction Process at Negative Potential: The electrochemical properties of the mononuclear complexes were studied by cyclic voltammetry in DMF solution containing 0.1 M TBAP as supporting electrolyte in the potential range 4.0 to −4.0 V. Figure 4 shows cyclic voltammogram of [L^3] and the reduction potential appeared on −1.80 V. Figure 5 shows cyclic voltammogram of Gd(III) ion and there is no reduction peack appeared in the range 0 to −2.0 V. Figure 6

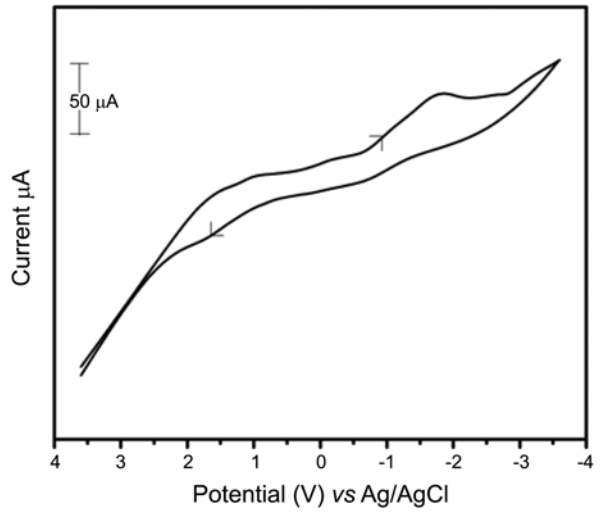

Figure 4. Cyclic voltammograms of L^3 ligand.

Table 2. Lifetime measurement value of mono nuclear [Gd(III)L^1-L^5]

Complexes	τ_1/ns	α_1 (%)	τ_2/ns	α_2 (%)	τ_3/ns	α_3 (%)	χ^2
[Gd(III)L^1]	0.736	12.72	2.577	38.91	7.743	48.38	1.037
[Gd(III)L^2]	0.730	12.66	2.591	25.73	8.759	61.61	0.964
[Gd(III)L^3]	0.775	12.94	2.305	34.95	8.286	52.11	1.090
[Gd(III)L^4]	0.634	19.84	2.068	45.44	7.859	34.72	0.988
[Gd(III)L^5]	1.113	29.23	2.913	33.80	8.583	36.98	1.198

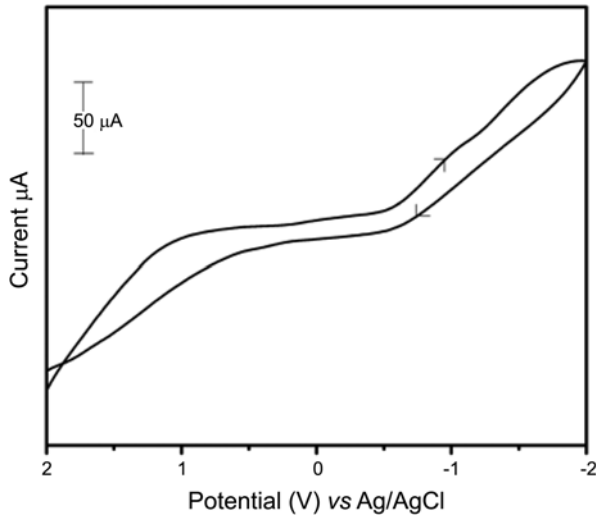

Figure 5. Cyclic voltammograms of $Gd(III)(NO_3)_3{\cdot}5H_2O$ metal solution.

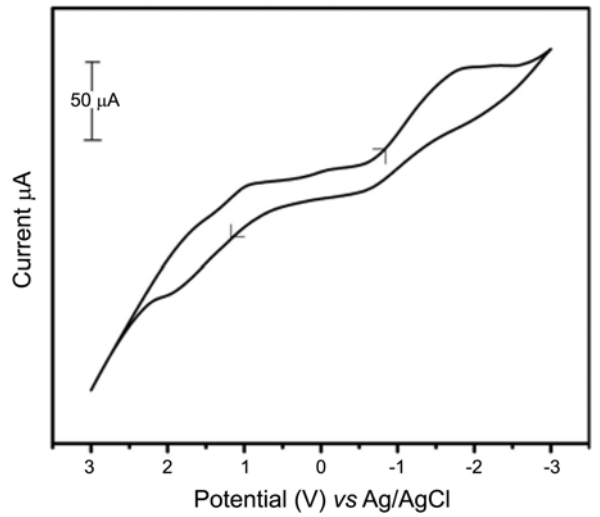

Figure 6. Cyclic voltammograms of $[Gd(III)L^3]$ complex.

shows cyclic voltammogram of $[Gd(III)L^3]$ complex and the reduction potential appeared at −1.80 V. Gd(III) ion is not getting reduced and only the ligands are involved in the reduction process. The electrochemical data of [Gd(III)L] complexes are given in Table 3(a). Generally the electrochemical properties of the complexes depend on a number of factors such as chelate ring/size, axial ligation, degree and distribution of unsaturation and substitution pattern in the chelate ring. Each voltammogram shows one electron irreversible reduction wave at a negative potential in the range −1.60 V to −2.15 V. The controlled potential electrolysis carried out at 100 mV more negative than the reduction wave conveys the consumption of one electron per molecule.

The electrochemical data shows that reduction potential of the complexes $[Gd(III)L^1]$ to $[Gd(III)L^5]$ shifts towards anodic direction from −2.15 V to −1.60 V. This shows that, when the number of methylene groups between the imine nitrogens (chain length) increases, the entire acyclic ring

Table 3. Electrochemical data for $[Gd(III)L^1\text{-}L^5]$ complexes [a]Reduction (at cathodic potential) and [b]Hydrolysis of 4-Nitrophenylphosphate data for the complexes

Complexes	[a]Reduction (at cathodic) (V)	[b]Rate constant (k) × 10^{-3} min^{-1} NPP
$[Gd(III)L^1]$	-2.15	2.33
$[Gd(III)L^2]$	-1.85	4.25
$[Gd(III)L^3]$	-1.80	5.34
$[Gd(III)L^4]$	-1.70	5.98
$[Gd(III)L^5]$	-1.60	7.63

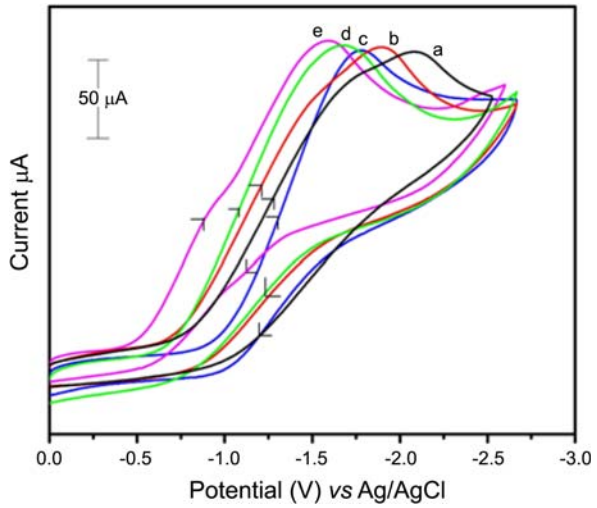

Figure 7. Cyclic voltammogram of $[Gd(III)L^1\text{-}L^5]$ complexes (Reduction potential). (a) $[Gd(III)L^1]$, (b) $[Gd(III)L^2]$, (c) $[Gd(III)L^3]$, (d) $[Gd(III)L^4]$ and (e) $[Gd(III)L^5]$.

becomes more flexible, which causes a distortion of the geometry of the gadolinium(III) complexes and makes the system more flexible.[23-25] The cyclic voltammogram are shown in Figure 7.

Kinetic Studies.

Hydrolysis of 4-Nitrophenylphosphate: The catalytic activity of the gadolinium(III) complexes on the hydrolysis of 4-nitrophenylphosphate was determined spectrophotometrically by monitoring the increase in the characteristic absorbance of the 4-nitrophenolate anion at 420 nm over the time in dimethylformamide at 25 °C. For this purpose, 10^{-3} mol dm^{-3} solutions of complexes in dimethylformamide were treated with 100 equivalents of 4-nitrophenyl phosphate in the presence of air. The course of the reaction was followed at 420 nm for nearly 45 min at regular time intervals. The slope was determined by the method of initial rates by monitoring the growth of the 420 nm band of the product 4-nitrophenolate anion. A linear relationship for all the complexes shows a first-order dependence on the complex concentration for the systems. Plots of log (Aα/Aα-At) versus time for hydrolysis of 4-nitrophenylphosphate activity of the complexes are obtained and shown in Figure 8. The inset in Figure 8 shows the time dependent growth of *p*-nitrophenolate chromophore in the presence of $[Gd(III)L^5]$. The

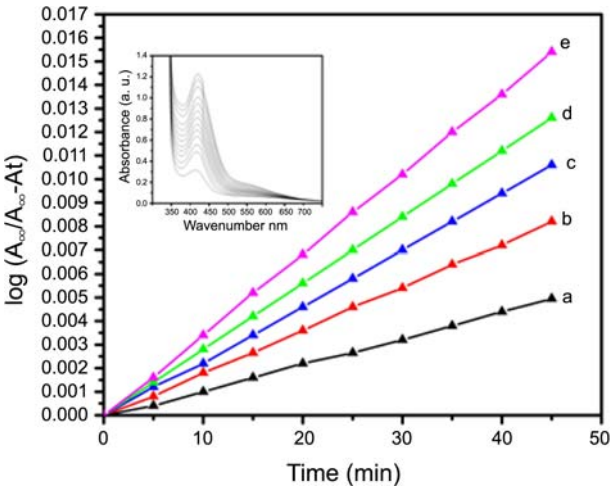

Figure 8. Catalysis of 4-nitrophenylphosphate by the [Gd(III)L^1-L^5] complexes: (a) [Gd(III)L^1], (b) [Gd(III)L^2], (c) [Gd(III)L^3], (d) [Gd(III)L^4] and (e) [Gd(III)L^5] The inset is the time dependent growth of *p*-nitrophenolate chromophore in the presence of [Gd(III)L^5].

observed initial rate constant values for all the Gd(III) complexes are given in Table 3(b). The catalytic activities of the Gd(III) complexes found to increase as the chain length increases due to the flexibility resulting from the distraction of the coordination sphere, *i.e.* increasing in the chain length enhances the rate constant of hydrolysis fairly well by producing distortion in the geometry around the metal ion that enhances the accessibility of the metal ion for the bonding of phosphate and OH groups.[26-28] The rate constant value for the mononuclear gadolinium complexes was found to be increasing in the following order:

$$[Gd(III)L^1] < [Gd(III)L^2] < [Gd(III)L^3] < [Gd(III)L^4] < [Gd(III)L^5]$$

Antimicrobial Activity. The bacterial inoculums was uniformly spread using sterile glass rod on a sterile Petri dish containing Nutrient Agar. Five concentrations of 25, 50, 75, 100 and 125 μM of pure substances were prepared in DMSO. The test substances of 50 μL were added to each of the 5 wells (7 mm diameter holes cut in the agar gel, 20 mm apart from one another). The systems were incubated for 24 h at 36 °C ± 1 °C, under aerobic conditions. After incubation, confluent bacterial growth was observed. Inhibition of the bacterial growth was measured in mm. Tests were performed in duplicate, whose minimum inhibitory concentration (MIC) values are provided in centimeters (cm) in diameter.

Antimicrobial activity of gadolinium(III) complexes against five tested microorganisms has been studied. As per the recorded data of [Gd(III)$L^{1\text{-}5}(NO_3)$] mono nuclear complexes showed different effects against the different organisms showing highest activity against *Klebsiella* sp. and at the

Table 4. Antibacterial activity of the test substances [Gd(III)L^1]

	[Gd(III)L^1]				
	25 μM	50 μM	75 μM	100 μM	125 μM
P. aeruginosa	0.67 ± 0.58	0.67 ± 0.58	0.67 ± 0.58	0.93 ± 0.057	1.67 ± 0.58
S. typhi	0.00 ± 0.00	0.00 ± 0.00	0.00 ± 0.00	0.00 ± 0.00	0.00 ± 0.00
C. albicans	0.67 ± 0.58	0.67 ± 0.58	0.67 ± 0.58	0.67 ± 0.115	0.90 ± 0.00
S. typhi Para A	0.67 ± 0.58	0.67 ± 0.58	0.60 ± 0.16	0.67 ± 0.58	1.67 ± 0.58
Klebsiella	0.67 ± 0.58	1.443 ± 0.057	1.47 ± 0.05	1.67 ± 0.00	1.7 ± 0.00

Table 5. Antibacterial activity of the test substances [Gd(III)L^2]

	[Gd(III)L^2]				
	25 μM	50 μM	75 μM	100 μM	125 μM
P. aeruginosa	0.00 ± 0.00	0.00 ± 0.05	0.30 ± 0.10	0.80 ± 0.10	0.64 ± 0.11
S. typhi	0.00 ± 0.00	0.00 ± 0.00	0.00 ± 0.00	0.00 ± 0.00	0.00 ± 0.00
C. albicans	0.00 ± 0.00	0.00 ± 0.00	0.00 ± 0.10	0.00 ± 0.05	0.10 ± 0.00
S. typhi Para A	0.00 ± 0.00	0.00 ± 0.05	0.00 ± 0.00	0.00 ± 0.00	0.00 ± 0.00
Klebsiella	0.64 ± 0.11	0.64 ± 0.11	0.67 ± 0.11	0.80 ± 0.10	1.20 ± 1.00

Table 6. Antibacterial activity of the test substances [Gd(III)L^3]

	[Gd(III)L^3]				
	25 μM	50 μM	75 μM	100 μM	125 μM
P. aeruginosa	0.00 ± 0.00	0.00 ± 0.00	0.00 ± 0.00	0.00 ± 0.00	0.00 ± 0.00
S. typhi	0.00 ± 0.00	0.00 ± 0.00	0.00 ± 0.00	0.00 ± 0.00	0.00 ± 0.00
C. albicans	0.00 ± 0.00	0.00 ± 0.00	0.00 ± 0.00	0.00 ± 0.00	0.67 ± 0.58
S. typhi Para A	0.00 ± 0.00	0.00 ± 0.00	0.64 ± 0.11	0.64 ± 0.11	0.64 ± 0.11
Klebsiella	0.00 ± 0.00	0.00 ± 0.00	0.00 ± 0.00	0.00 ± 0.00	0.00 ± 0.00

Table 7. Antibacterial activity of the test substances [Gd(III)L^4]

	[Gd(III)L^4]				
	25 μM	50 μM	75 μM	100 μM	125 μM
P. aeruginosa	0.00 ± 0.00	0.00 ± 0.00	0.00 ± 0.00	0.00 ± 0.00	0.60 ± 0.10
S. typhi	0.00 ± 0.00	0.00 ± 0.00	0.00 ± 0.00	0.00 ± 0.00	0.60 ± 0.10
C. albicans	0.00 ± 0.00	0.00 ± 0.00	0.00 ± 0.00	0.00 ± 0.00	0.60 ± 0.05
S. typhi Para A	0.00 ± 0.00	0.00 ± 0.00	0.00 ± 0.00	0.00 ± 0.00	0.60 ± 0.05
Klebsiella	0.80 ± 0.10	1.00 ± 0.58	1.00 ± 0.11	1.11 ± 0.00	1.8 ± 0.05

Table 8. Antibacterial activity of the test substances [Gd(III)L^5]

	[Gd(III)L^5]				
	25 μM	50 μM	75 μM	100 μM	125 μM
P. aeruginosa	0.80 ± 0.10	1.00 ± 0.58	1.20 ± 1.11	1.20 ± 0.00	1.6 ± 0.05
S. typhi	0.00 ± 0.00	0.00 ± 0.00	0.00 ± 0.00	0.00 ± 0.00	0.00 ± 0.00
C. albicans	0.00 ± 0.00	0.00 ± 0.00	0.60 ± 0.10	0.60 ± 0.10	0.60 ± 0.05
S. typhi Para A	0.00 ± 0.00	0.60 ± 0.10	0.60 ± 0.10	0.60 ± 0.10	0.60 ± 0.05
Klebsiella	0.64 ± 0.11	0.70 ± 0.11	0.71 ± 0.115	0.80 ± 0.10	0.84 ± 0.11

concentration of 125 μM. Complex [Gd(III)$L^1(NO_3)_2$] and [Gd(III)$L^{5a}(NO_3)$] have the highest antimicrobial activity against five organisms data are given in the Tables 4 to 8. In contrast [Gd(III)L^{3a}] showed the lowest activity. MIC of Nutrient agar plates photos are given as supplementary Figure S3.1 to S3.5 While the cell walls of fungi contain chitin, the cell walls of bacteria contain murein. In addition, fungi contain ergosterol in their cell membranes instead of the cholesterol found in the cell membranes of animals. In addition, the difference in the antibacterial activity of gadolinium(III) complexes studied in this work probably is associated to ligand type and its space distribution around the complex core. This difference might be due to different structure of complex and activity of imine nitrogen *i.e.* difference in binding sight of ligands with the molecules.[29-31]

Conclusion

Five Schiff-base gadolinium(III) complexes have been synthesized and their antimicrobial activity have been investigated. The electronic spectra indicate that all mono nuclear [Gd(III)L] complexes have distorted mono-capped square antiprism geometry and the observed red shift in the spectra is due to the increase in chain length. Fluorescence emission of Gd(III) ions in the complex was influenced by the ligand center. All the mono nuclear [Gd(III)L^1-L^5] complexes have tri exponential decay cure fitting. In particular, [Gd(III)L^5] complex have higher life time value. Cyclic voltammograms exhibit one electron irreversible process. The observed shift of reduction potential towards anodic direction was due to increasing chain length. The complexes show higher catalytic activity on increasing chain length. Complex [Gd(III)L^5] have higher antimicrobial activity than the other complexes which is due to the longer chain length of the imine compartment. All these studies of the complexes agree well with the established trend.

Supplementary Material. FT IR spectra of [Gd(III)L^1], [Gd(III)L^2], [Gd(III)L^3], [Gd(III)L^4] [Gd(III)L^5] complexes, ESI Mass spectra of [Gd(III)L^4], [Gd(III)L^5] complexes and Antimicrobial activity (Minimum Inhibitory Concentration) data of complexes [Gd(III)L^1], [Gd(III)L^2], [Gd(III)L^3], [Gd(III)L^4], [Gd(III)L^5] MIC of Nutrient agar plates photos have given as supplementary material.

Acknowledgments. Financial support from CSIR, New Delhi is gratefully acknowledged and we acknowledged National Centre for Ultrafast Process, University of Madras, for the lifetime measurements.

References

1. Nelson, J.; McKee, V.; Morgan, G.; Karlin, K. D. Ed., *Progress in Inorganic Chemistry*; Wiley: New York, 1988; Vol. 47, p 47.
2. (a) George, S. M.; Hwan Yon, G.; Keun Park, B.; Mun Lee, K.; Do, Y.; Gyoun Kim, C.; Chung, T.-M. *Bull. Korean Chem. Soc.* **2012**, *33*, 2059. (b) Rudkevich, D. M.; Mercer-Chalmers, J. D.; Verboom, W.; Ungaro, R.; De Jong, F. *J. Am. Chem. Soc.* **1995**, *117*, 6124.
3. Evans, C. H. *Biochemistry of Lanthanide*; Plenum: New York, 1990.
4. Lauffer, R. B. *Chem. Rev.* **1987**, *87*, 901.
5. Aime, S.; Botta, M.; Fasano, M.; Terreno, *E. Chem. Soc. Rev.* **1998**, *27*, 19.
6. Tweedle, M. F. *Invest. Radiol.* **1992**, *27*, 2.
7. (a) Werts, M. H. V.; Verhoeven, J. W.; Hofstraat, J. W. *J. Chem. Soc., Perkin Trans.* **2000**, *2*, 433. (b) Beeby, A. B.; Dickins, R. S.; Faulkner, S.; Parker, D.; Williams, J. A. G. *Chem. Commun.* **1997**, 1401.
8. Morrow, J. R.; Buttrey, L. A.; Shelton, V. M.; Berback, K. A. *J. Am. Chem. Soc.* **1992**, *114*, 1903.
9. Sink, R. M.; Buster, D. C.; Sherry, A. D. *Inorg. Chem.* **1990**, *29*, 3645.
10. Ramasamy, R.; Mota de Freitas, D.; Jones, W.; Wezeman, F.; Labotka, R.; Geraldes, C. F. G. C. *Inorg. Chem*. **1990**, *29*, 3979.
11. (a) Hwa Han, S.; Nu Zheng, Z.; Cho, S.; Lee, S. W. *Bull. Korean Chem. Soc.* **2012**, *33*, 2017. (b) Dick, L. R.; Geraldes, C. F. G. C.;

Sherry, A. D.; Gray, C. W.; Gray, D. M. *Biochemistry* **1989**, *28*, 7896.
12. Gunnlaugsson, T.; Mac Dónail, D. A.; Parker, D. *Chem. Commun.* **2000**, 93.
13. Piguet, C.; Bunzli, J. C. G. *Chem. Soc. Rev.* **1999**, *28*, 347.
14. Freire, R. O.; Rocha, G. B.; Simas, A. M. *J. Mol. Model* **2006**, *12*, 373.
15. Duff, J.C. *J. Chem. Soc.* **1941**, 547.
16. Vijayaraj, A.; Prabu, R.; Suresh, R.; Sivaraj, C.; Raaman, N.; Narayanan, V. *J. Coord. Chem.* **2011**, *64*, 637.
17. Vijayaraj, A.; Prabu, R.; Suresh, Jayanthi, G.; Muthumary, J.; Narayanan, V. *Synthesis and Reactivity in Inorganic, Metal-Organic, and Nano-Metal Chemistry*, **2011**, *41*, 963.
18. Nakamoto, K. *Infrared Spectra of Inorganic and Coordination Compounds*; John Willey and Sons: New York, 1986; p 244.
19. Li, X.; Wanyan, H.; Dong, W.; Yang, R. *Polyhedron* **1990**, *9*, 2285.
20. Li, X.; Wanyan, H.; Dong, W.; Yang, R. *Polyhedron* **1993**, *12*, 2021.
21. Dawson, W.; Kropp, J.; Windsor, M. *J. Chem. Phys.* **1966**, *45*, 2410.
22. Asiri, A. M.; Khan, S. A.; Al-Amoudi, M. S.; Alamry, K. A. *Bull. Korean Chem. Soc.* **2012**, *33*, 1900.
23. Bareford, G. K.; Freeman, G. M.; Erver, D. G. *Inorg. Chem.* **1986**, *86*, 552.
24. (a) Bowmaker, G. A.; Williams, J. P. *J. Chem. Soc., Dalton Trans.* **1993**, 3593. (b) Gao, E.; Bu, W.; Yang, G.; Liao, D.; Jiang, Z.; Yan, S.; Wang, G. *J. Chem. Soc., Dalton Trans.* **2000**, 1431.
25. Prabu, R.; Vijayaraj, A.; Suresh, R.; Jagadish, L.; Kaviyarasan, V.; Narayanan, V. *Bull. Korean Chem. Soc.* **2011**, *32*, 1669.
26. Jurek, P. E.; Jurek, A. M.; Martel, A. E. *Inorg. Chem.* **2000**, *39*, 1016.
27. Sreedaran, S.; Bharathi, K. S.; Rahiman, A. K.; Rajesh, K.; Nirmala, G.; Jagadish, L.; Kaviyarasan, V.; Narayanan, V. *Polyhedron* **2008**, *27*, 1867.
28. Sreedaran, S.; Bharathi, K. S.; Rahiman, A. K.; Jagadish, L.; Kaviyarasan, V.; Narayanan, V. *Polyhedron* **2008**, *27*, 2931.
29. Ben Arfa, A. *Lett. Appl. Microbiol.* **2006**, *43*, 149.
30. Almeida, A. A. *J. Agric. Food Chem*. **2006**, *54*, 8738.
31. Brenda, M.; Rene, T.; Marcela Urzua, W. *J. Chil. Chem. Soc.* **2004**, *49*, 1.